Scalable Computing: Practice and Experience, ISSN 1895-1767, http://www.scpe.org
© 2024 SCPE. Volume 25, Issues 4, pp. 2985–3000, DOI 10.12694/scpe.v25i4.2939

CONSTRUCTION AND APPLICATION OF THREE-DIMENSIONAL INFORMATION MANAGEMENT SYSTEM FOR INTELLIGENT BUILDINGS INTEGRATING BIM AND GIS TECHNOLOGIES

JING SHI*

Abstract. Smart building technologies are widely used in all aspects of building structure, services, and management, helping to create a more comfortable, safe and convenient building environment. Building Information Modelling (BIM) and Geographic Information System (GIS) technologies are both widely used intelligent building technologies, and their combination can improve the analytical ability of spatial environment to a certain extent. However, it is difficult to manage them due to the huge amount of data in the Three-Dimensional (3D) information of intelligent buildings. Therefore, it is very important to improve the information management ability of intelligent building 3D information management systems (Moballeghi et al. 2023; Mahamood and Fathi 2022). BIM and GIS technologies were used to build a 3D information management system for intelligent buildings more effectively. The design and development principles of the information management system were explained, and the overall framework of the system was also designed. Research was conducted on feature extraction and matching through an improved scale invariant feature transformation algorithm to enhance the information classification and management capability of the intelligent building 3D information management system. In addition, the improvement measure for SIFI algorithm was to reduce pixel processing to reduce its memory size. The study explained the preprocessing of model normalization before feature extraction and matching. The coordinate system rotation normalization of building 3D models was achieved through principal component analysis. Finally, the calculation of covariance matrix was explained. The number of pyramid image groups was adopted to further improve the scale space and enhance computational efficiency. The Hessian matrix was introduced to eliminate unstable fixed points. And the purity of feature point matching through similarity coefficients was improved. In addition, a modified multi-view convolutional neural network was used to classify the feature data, and a modified classification architecture was designed to build a 3D model based on this algorithm to enhance its information classification management capabilities. The study explained the calculation of view weights and global descriptors and described the fully connected and classification architectures. The results showed that the improved scale-invariant feature conversion algorithm achieved a matching accuracy of 98.3% and takes only 17 s. Meanwhile, the proposed multi-view convolutional neural network achieved an accuracy of 97.6% and an F1 value of 96.4% for the classification of 3D information of intelligent buildings. Among the six types of 3D building models selected, the method achieved the highest accuracy of 94.26% and was more stable. It shows that the proposed method of 3D information management of intelligent buildings has obvious classification advantages and provides a new technical reference for the information development of intelligent buildings.

Key words: BIM; GIS; Intelligent buildings; 3D information; Management systems; Multi-view convolutional neural networks

1. Introduction. Introduction. With the gradual development of digital city construction, intelligent buildings have become a key focus of development [31, 24] . As the focal point of modelling technology in the construction industry, Building Information Modelling (BIM) enables the integration of information from planning, decision making, and design aspects of construction projects, thus enhancing economic, social, and environmental benefits to a certain extent [30, 32]. BIM mainly uses 3D digital simulation techniques to construct buildings and simulate realistic situations. The technology also enables information sharing between the various participants in a project on the same platform to facilitate their communication and decision-making. However, BIM technology has inherent drawbacks such as the small spatial scope, which makes it difficult to integrate building facilities into the environment [42, 36] Geographic Information System (GIS) technology, on the other hand, uses geospatial data of the earth as an object. When integrated with BIM technology, it can enhance the analysis of the spatial environment. However, in today's intelligent buildings, it is difficult to achieve efficient management due to the complexity of the data contained in 3D information and the excessive amount of data [38, 18]. Therefore, BIM is used for building modelling and imports it into

*Department of Engineering Management, Henan Technical College of Construction, Zhengzhou 450000, China (Corresponding author, (jingshisj@outlook.com)

GIS for visual presentation. The improved Scale-Invariant Feature Transform (SIFT) is also applied to extract and match the features of the 3D images of intelligent buildings, and the improved Multi-View Convolutional Neural Network (MVCNN)-based Deep Convolutional Neural Network (DCNN) is used. The research aims at building intelligent building 3D information management systems by combining BIM and GIS technologies, and reducing the difficulty of system management through SIFI and MVCNN. The research also aims to improve the information classification management ability of the system, provide technical support for the efficient management of intelligent building 3D information, and promote the informatization development of intelligent building. The novelty of the research is mainly reflected in four aspects. The first aspect is the introduction of the improved SIFI algorithm in the building 3D information management system. It can reduce the memory size and the computational cost of the overall process by downsizing the pixel processing, realize the feature extraction matching of the building 3D information, and reduce the memory occupation of the 3D building information. The second aspect is the adoption of the modified MVCNN, which is improved by the introduced weight calculation module. As a result, the features of multiple views are fused, the accuracy of 3D model data classification is improved, and the information management capability of the system is enhanced. The third aspect is the introduction of the Long Short-Term Memory (LSTM) and the Attention Mechanism (Att) module, through which the weight calculation is performed. The fourth aspect combines the improved SIFI and MVCNN modes, which are applied to improve the management ability of the intelligent building 3D information management system. The contribution of this research is to improve the accuracy of data classification for intelligent building 3D models and reduce the computational complexity of the overall process of 3D information feature extraction and matching. The information management capability of intelligent building 3D information management systems is enhanced and the technical and methodological support is provided for the informatization and intelligent development of intelligent buildings. The study consists of four parts. The first part is a DCNN based on the improved Multi-View Convolutional Network (MVCNN), which provides a research status on BIM-GIS integration technology and classification of 3D images. The second part explains in detail the construction of a 3D Information Management (IM) system for buildings by integrating BIM and GIS and the processing of system data. Section 1 of the second part introduces the construction of the 3D IM system by integrating BIM and GIS technologies. Section 2 focuses on the feature extraction and classification processing of the data of the management system. The third section discusses the performance of each algorithm and the effectiveness of applying each technique. The fourth part discusses the results obtained and explores future directions for improvement.

2. Related works. [1] had developed an integrated BIM-GIS model for the manufacturing and management of buildings. BIM was applied for the production, analysis, and management of building information. GIS was applied for the 3D model creation. The results showed that the model had excellent practical application and could be used to select the best location for the construction of warehouses. [11] introduced an integrated approach of BIM and GIS to achieve a more intelligent urban management. CIM models were used to enhance the intelligent management of the city. The results showed that this approach could effectively solve the management problems in infrastructure development projects. [39] addressed the data conversion problems associated with urban geotagging languages. A shapefile format was adopted to facilitate the application of BIM models in GIS, and a method was developed to convert industry base classes into shapefiles using integrated computer graphics technology. The results showed that the method could promote the application of BIM in GIS and facilitate integrated building model construction. [23] explored 24 BIM applications in the lifecycle and explored BIM applications and integration techniques from two perspectives to provide a systematic summary of BIM integration, applications, and trends. The results showed that the technology provided effective technical support for various fields in the future. [37] proposed a new approach to integrate BIM with GIS in response to the problems of large scale and technical complexity that construction projects had. A web-based integration platform was also developed to enhance building information sharing and facilitate project management. The results showed that it was effective in enabling the proper management of large projects. The problem of classifying 3D images has been the topic of much research. [32] found that current 3D model classification relied heavily on fully supervised training schemes. Therefore, a semantically guided projection method was proposed for retrieving and classifying 3D models. A bidirectional projection of visual features and semantics was also used to eliminate the difference between the visible and invisible domains. It

was highly feasible according to the findings [5]. [10] designed an in-situ measurement method based on a binocular microscopic vision system to measure the size distribution of 3D crystals during the crystallization. The shape of 3D particles was reconstructed through dual view images captured by two microscopic cameras. In addition, a microscopic dual view image analysis method was also designed to identify key corner points of particle shape in the image. The experimental results showed that the method designed by the research institute could effectively estimate the 3D size of particles and had good performance. [36] proposed an interpretable machine learning method for point cloud classification to classify 3D building model images. In the classification and integration stages, multiple point-hopping units were employed to acquire feature vectors and provide them to the classifier. The method had good classification performance according to the findings. [38] proposed a new 3D efficiency net with improved 3D moving inverse bottleneck convolution blocks for classification detection of 3D images of Alzheimer's disease to achieve classification of brain MR images. It could effectively perform the prediction and diagnosis of Alzheimer's disease according to the findings. [18] developed a new street frontage network to design urban elements that were more conducive to public space to enable quality assessment of street frontages. It was 92% accurate and could be applied to the design of urban elements according to the findings. In summary, domestic and foreign research scholars have implement extensive research on the management of building information and the classification of 3D images, but there is still room for further research and improvement on the classification of 3D images of buildings. Therefore, the study builds a building 3D IM system rely on BIM and GIS technologies, and classifies the system data effectively, in order to achieve a more intelligent system management.

3. Intelligent building three-dimensional IM under the integration of BIM and GIS technologies. Intelligent buildings mainly rely on modern computer technology. A 3D building IM system based on BIM and GIS integration technology is constructed in this section. Meanwhile, a modified scale-invariant feature conversion algorithm is introduced for pixel reduction to address the complexity and excessive memory of the system data. In addition, an improved MVCNN method is proposed to classify the data after feature matching to achieve a more refined and intelligent building IM.

3.1. Construction of 3D IM system based on BIM and GIS technologies. BIM models are able to achieve access to information about the interior and exterior structures of a building through 3D digital information. However, the space in which they are applied is too narrow and susceptible to architectural and geographical conditions, resulting in building facilities not being integrated into their environment. GIS has advantages in this area, as it takes the geospatial data of the whole earth as an object and performs a series of technical operations on it [20] GIS is now widely used in the field of exterior spatial planning and location selection of buildings. The integration of 3D BIM models with GIS platforms not only enriches the macro to micro building information, but also effectively deals with the problem of information silos from micro to macro [6, 9] The integration of both data can give full play to their respective strengths and make up for their weaknesses to achieve a more complete 3D model of the building and its surroundings. By combining BIM and GIS technologies, the 3D building IM system enables intelligent buildings to manage and maintain projects throughout their lifecycle. Meanwhile, visual displays and spatial analysis conditions are provided to achieve an increased level of intelligence and energy efficiency in intelligent buildings, saving resources and improving efficiency to a certain extent. The development phase of the 3D IM system for intelligent buildings should be based on certain design and development principles for successful construction. The study identifies six construction principles, namely security, advanced practicality, reasonable openness, standardization, scalability, and unified design, to ensure the successful construction of the 3D IM system. The principle of security is extremely important and refers to the protection of data and information in a system against information theft. The principle of advanced practicality means that the choice of technologies needs to be in line with the current mainstream technologies and meet future development trends. The principle of reasonable openness means that both the development environment and the hardware support diversity to adapt to changes in operating systems and computers [28, 4] The principle of standardization refers to the need for a unified standard specification to ensure compatibility and interoperability. The principle of scalability means that a certain number of upgrade interfaces must be reserved to meet upgrade and expansion needs, while ensuring the interoperability of the system. The principle of uniformity of design is to ensure uniformity for all parts of the system and the architecture and achieve uniform planning and design [36, 26] The role of the six construction

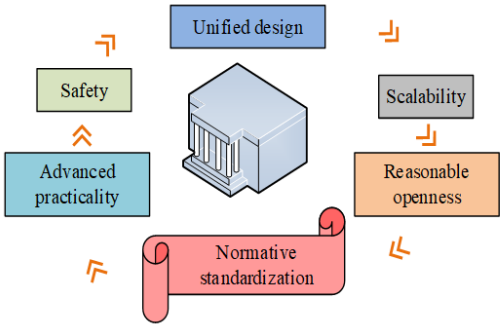

Fig. 3.1: The role of the six construction principles identified in the construction of a three-dimensional IM system

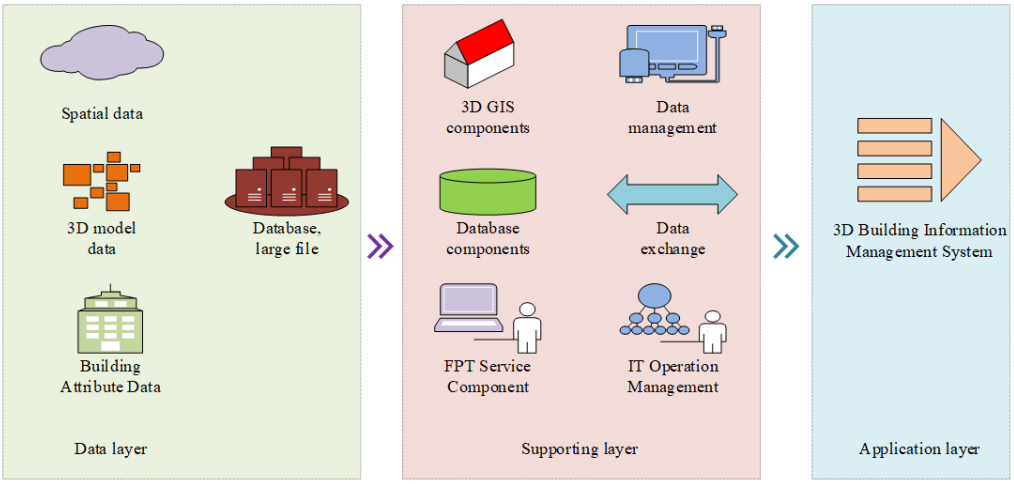

Fig. 3.2: The overall framework of intelligent building 3D IM system proposed by the research institute

principles identified in the study in the construction of the 3D IM system is shown in Figure 3.1.

The overall objective is to build a digital 3D simulation model containing architectural information with buildings and components, including manual mapping, point clouds, images, and other information. The system manages the texture data and geometric models of building complexes, and data are also aggregated on architectural artefacts, including architectural images, documents, and audio. The system allows users to fully understand the properties and spatial information of the building and its components to better manage and make decisions about the building in a systematic way, leading to a more scientific IM of the building archive. The overall structure of the proposed 3D IM system for intelligent buildings contains three parts, namely the data layer, the support layer, and the application layer, as shown in Figure 3.2.

In Figure 3.2, the bottom layer is the data layer, which mainly includes the data of the 3D model, spatial, and attribute of the building. The storage of such data is generally achieved by establishing a database or large files. Meanwhile, the support layer of the system contains two main aspects: the components and the management and exchange of data. The role of the data management and exchange layer is to provide the application layer with the ability to download, store, utilize, manage, and exchange data. The role of the component layer is to provide a variety of platforms for the development and operation, including the 3D GIS platform, database platform, and FTP service platform. In addition, the application layer is used to develop

efficient applications for the 3D building IM system to complete building IM.

3.2. Intelligent building 3D IM based on data classification. The integration of BIM and GIS provides rich data support, enabling more refined management of 3D information for smart buildings and enabling intelligence of micro-information. However, the data obtained from BIM and GIS technologies have the characteristic of high resolution, which occupies a large amount of memory and brings greater difficulties for the next data management [7] For this reason, an improved SIFT algorithm is introduced, which is pixel-reduced to reduce the memory size. At the same time, the data in the IM system are classified by the improved data classification algorithm to achieve efficient management. The model is pre-processed with a normalized coordinate system before feature extraction and matching. This includes translation normalization, rotation normalization, and scale normalization of the coordinate system. The gravity center of the model is shifted to the origin of the coordinate system to achieve normalization. The x-axis coordinates of the centre of gravity of the model are calculated as shown in equation 3.1 [14, 16].

$$x_c = \frac{\sum_{i=0}^{m-1} x_i}{m} \tag{3.1}$$

In equation 3.1,x_i represents the x-axis coordinates of the model midpoint i, and the y-axis coordinates of the model centre of gravity are calculated as shown in equation equation 3.2.

$$y_c = \frac{\sum_{i=0}^{m-1} y_i}{m} \tag{3.2}$$

In equation 3.2,y_i represents the y-axis coordinates of the model midpoint i, and the z-axis coordinates of the model centre of gravity are calculated as shown in equation 3.3 .

$$z_c = \frac{\sum_{i=0}^{m-1} z_i}{m} \tag{3.3}$$

In equation 3.3, z_i represents the z-axis coordinates of the point i in the model. The converted coordinates are shown in equation 3.4.

$$P_i' = (x_i - x_c, y_i - y_c, z_i - z_c) \tag{3.4}$$

The rotation normalization of the coordinate system of the architectural 3D model is mainly achieved through principal element analysis, which first requires the calculation of the covariance matrix, which is shown in equation 3.5 [33].

$$C = \left| \begin{array}{ccc} \sum_{k=0}^{m} x^2 & \sum_{k=0}^{m} xy & \sum_{k=0}^{m} xz \\ \sum_{k=0}^{m} xy & \sum_{k=0}^{m} y^2 & \sum_{k=0}^{m} yz \\ \sum_{k=0}^{m} xz & \sum_{k=0}^{m} yz & \sum_{k=0}^{m} z^2 \end{array} \right| \tag{3.5}$$

The matrix is a real symmetric matrix with non-negative real eigenvalues. The eigenvalues are then placed in a non-increasing order.

The feature vectors are sorted to obtain the feature vectors. The feature vectors are then scaled to produce a rotation matrix, and a rotation transformation of all the points of P' in the model will result in a new set of points, which is calculated as shown in equation 3.6 (Liu. 2022).

$$P'' = \{P_l'' \,|\, P_l'' = P_l' R,\ P_l' \in P^i,\ l = 0, 1, ..., m\} \tag{3.6}$$

After the rotational transformation, it is then necessary to carry out a scale normalization of the coordinate system, which is calculated as shown in equation 3.7 [19].

$$P''' = \left\{ \frac{x_s''}{r_{\max}}, \frac{y_s''}{r_{\max}}, \frac{z_s''}{r_{\max}} \,\middle|\, |(x_s'', y_s'', z_s'')_s\rangle \right\} \tag{3.7}$$

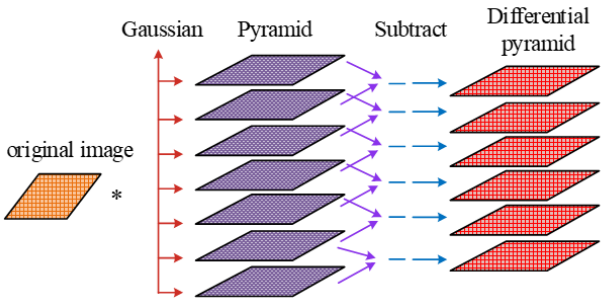

Fig. 3.3: The construction process of Gaussian difference pyramid

Once the data of the architectural 3D model have been pre-processed, the model features are extracted and assigned. The SIFT algorithm consists of four computational steps, namely the construction of a scale space, the detection of feature points, the assignment of key point principal directions, and the calculation of feature descriptors. Building a multi-scale space means extracting effective visual processing information from the changing scale parameters, while aggregating them to achieve deep mining of the essential features of the image. The feature points of the image can be better extracted when a multi-scale spatial transformation is applied to the target image [40, 3]. The scale transformation of an image is mainly achieved through a Gaussian convolution kernel, which is calculated as shown in equation 3.8 (YANG et al. 2021; Rathore et al. 2019).

$$\begin{cases} G(x,y,\sigma) = \frac{1}{2\pi\sigma^2} e^{\left(\frac{-(x^2+y^2)}{2\sigma^2}\right)} \\ L(x,y,\sigma) = G(x,y,\sigma) \otimes I(x,y) \end{cases} \tag{3.8}$$

In equation 3.1, σ represents the scale factor, $G(x,y,\sigma)$ is a two-dimensional Gaussian function, $I(x,y)$ refers to the input image, $\otimes$ stands for the convolution operation between images, and $L(x,y,\sigma)$ represents the scale space image after Gaussian convolution. When constructing the scale space, the Gaussian convolution function is used to generate a Gaussian pyramid with different scales, and then the two adjacent layers of this pyramid will be differentiated to be able to obtain a Gaussian differential pyramid, as shown in Figure 3.3.

Due to the huge amount of intelligent building image data collected, further improvement of the scale space is needed to enhance the computational efficiency. The number of pyramid image groups $(Octave, O)$ is reduced to achieve this purpose. The calculation of O is shown in equation 3.9 [27].

$$O = \log_2 (\min(M, N)) \tag{3.9}$$

In equation (3.9), $\{\}$ represents the rounding operation. M and N stand for the number of rows and columns in the image, respectively. If the first 2 sets of images are used for feature point extraction, $O = 2$ is applied to achieve improvement. Once the differential Gaussian pyramid has been generated, the detection of the feature points is performed. Typically, a point in the image is determined to be a polar point of the image if it is a minimal or maximal point in the full range of domains corresponding to that layer and neighbouring layers. The unstable points are eliminated by means of a Hessian matrix to eliminate the edge effects that occur in this process, and a similarity coefficient is introduced to improve the purity of feature point matching. The similarity coefficients are shown in equation (3.10) [41].

$$SC = \frac{dist}{Min\_dist} (1 \le SC \le SC\_\max) \tag{3.10}$$

In equation (3.10), Min_dist represents the minimum Euclidean distance and $SC\_\max$ is the maximum value of the similarity coefficient. If the obtained similarity coefficient is small, it means that the similarity between the pixel points of the same name is greater, which acts as a purification of the matched points. The

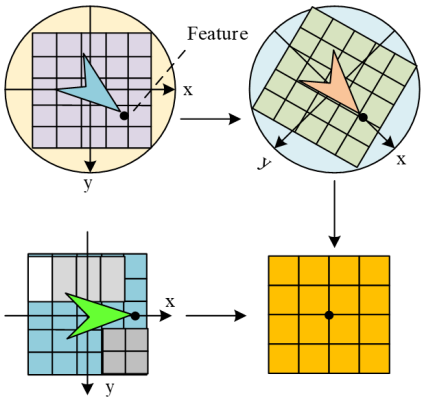

Fig. 3.4: Expression of feature direction

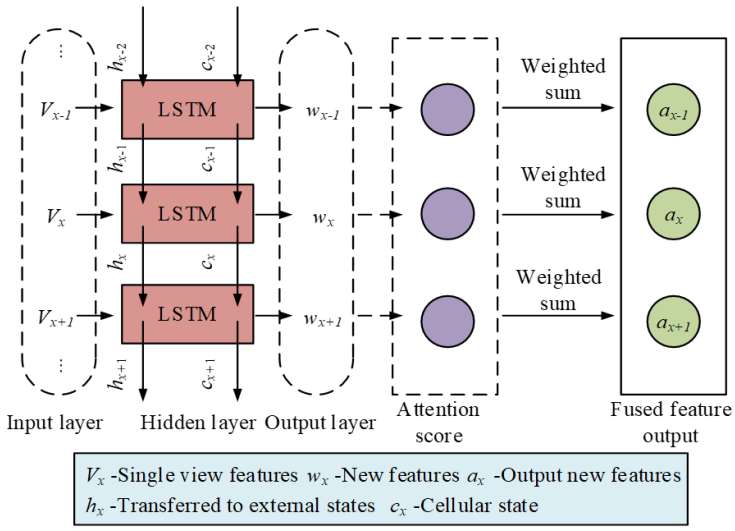

Fig. 3.5: The architecture of LSTM-Att module

direction, scale, and position of the feature points are usually described using a vector approach, as shown in Figure 3.4.

After completing the extraction and matching of model features, the deep convolutional neural network based on the modified MVCNN is improved to achieve data classification of architectural 3D models. Five convolutional layers and three fully connected layers form a network structure. The input of the network is six three-channel images, and the output is the shape descriptor of the 3D architecture model. To improve the classification detection performance of MVCNN on similar building components, the model is improved by adding weight calculation modules for each view after the main five convolutional layers of the network, thus giving different weights to the more expressive and less expressive views, respectively. The newly introduced weight calculation module is an LSTM-Att module that combines LSTM and Att. LSTM can accurately capture sequential features by utilizing the spatial correlation of multi-view images. Att can subjectively place weights during model training, ignoring irrelevant information, and thereby improving classification efficiency. The architecture of the LSTM-Att module is shown in Figure 3.5.

From Figure 3.5, the LSTM-Att module includes an input layer (single-view features), a hidden layer, an

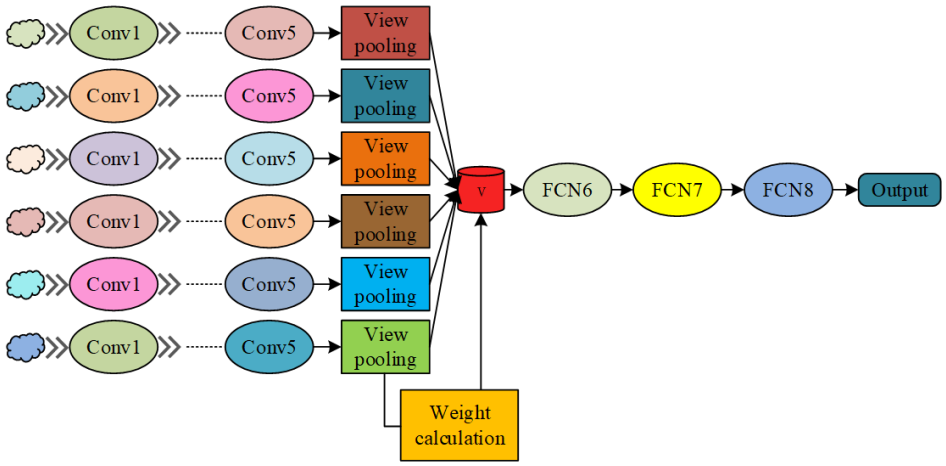

Fig. 3.6: Improved architecture for 3D model classification based on the improved MVCNN

output layer (new features), attention score, weighted summation, LSTM, and a fused feature output layer. LSTM-Att uses LSTM to accurately process multi-view feature data and obtain more complete features. Afterwards, the processed data are computed based on attention value, and multi-view feature fusion is performed based on weight data to improve classification accuracy. The modified architecture of the improved MVCNN-based 3D model classification is shown in Figure 3.6.

In Figure 3.6, the six views generated by the pre-processed model are first fed into the convolutional neural network for parallel convolution, and the original view descriptors for each view are obtained after the initial extraction of features for each of the six views. The original view descriptors are then fed into the weighting layer to give higher weights to the more expressive descriptors and lower weights to the less expressive descriptors. It is assumed that the input view is represented by equation 3.11.

$$T = \{I_1, I_2, I_3, ..., I_n\} \tag{3.11}$$

The differentiation of each view is calculated as shown in equation 3.12.

$$Q(I_n) = sigmoid(abs(C_n)) \tag{3.12}$$

In equation (3.12), C_n is the output value of the convolution layer (Hosseini and Taleai 2021). The weights are calculated as shown in equation (3.13) (Kaiwen et al. 2023).

$$H(I_n) = \frac{Ceil(|G_n| \times Q(I_k))}{|G_n|}, \qquad I_k \in G_n \tag{3.13}$$

In equation 3.13, G_n represents a view group. The groups of views are then pooled to generate global descriptors, where the global descriptors are calculated as shown in equation 3.14 (Kaczorek and Ruszewski 2022).

$$V(T) = \frac{\sum_{n=1}^{6} H(I_n) \cdot J_n}{\sum_{n=1}^{6} H(I_n)} \tag{3.14}$$

In equation 3.14, j_n represents the descriptors obtained by pooling. The resulting global descriptors then need to be fed into the fully connected layer to enable the classification of the building 3D model. One of the full connectivity and classification architectures is shown in Figure 3.7.

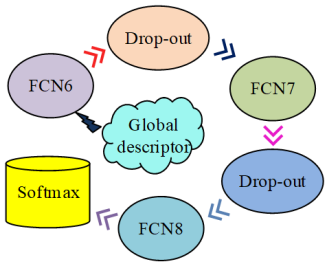

Fig. 3.7: Fully connected and classified architecture

Table 4.1: The experimental basic environmental parameters

Parameter variables	Parameter selection
CPU	Intel 8 CoreTM i7-7700HQ CPU
Memory	16G
GPU	NVIDIA Tesla P4*2
Implementation Platform	Ubuntu 16.04.6 LTS
Operating system	64 bit Wndows10
Operating environment	MATLAB
Data regression analysis platform	SPSS 26.0

Softmax and multi-classification are used for the classification of image features. The Softmax function is shown in equation 3.15.

$$S_i = \frac{e^{v_j}}{\sum_{i=1}^{C} e^{v_j}} \tag{3.15}$$

In equation 3.15, j represents the category index, v_j represents the output of the classifier's preceding output unit, and C is category quantity. S_i stands for the ratio of the output element index to the sum of all element indexes.

4. Analysis of the application effect of three-dimensional IM system for intelligent buildings.. Three feature extraction algorithms were selected to compare their performance to verify the effectiveness of the improved SIFT. These include ASIFI, BRISK, and the classical SIFT algorithm. Table 4.1 depicts the basic software and hardware environment settings.

The selected dataset is the UrbanScene3D dataset, which contains 16 building scenes and 128,000 high-resolution images. 1026 images of a building were taken as the test objects. Figure 4.1 shows the comparison results of the correct matching rate and time of the four algorithms. From Figure 8, the improved SIFT algorithm had the highest matching accuracy and was as high as 98.3%. Compared with the remaining algorithms, its matching accuracy rates were improved by 29.8%, 31.1%, and 37.6%, respectively. Meanwhile, the improved SIFT had the lowest matching time of 17s, which was 154s, 71s, and 192s less than the other algorithms, respectively, indicating that the improved SIFT algorithm had very good performance.

Figure 4.2 shows the results of the four methods in this dataset. From Figure 4.2a, in terms of the search completion rate, the difference between ASIFI and the classical SIFT algorithm was relatively small, with the lowest being around 50% and the highest close to 90%, and the overall trend was first decreasing and then increasing. In contrast, the improved SIFT algorithm was able to maintain a full rate above 78% and reached a maximum of 97%, a maximum improvement of 42% compared to the pre-improvement SIFT algorithm. In Figure 4.2b, the trends of the four methods were relatively close to each other, with the ASIFI, classical SIFT and BRISK algorithms all obtaining a relatively low maximum accuracy rate in the range of 40%-50%. The

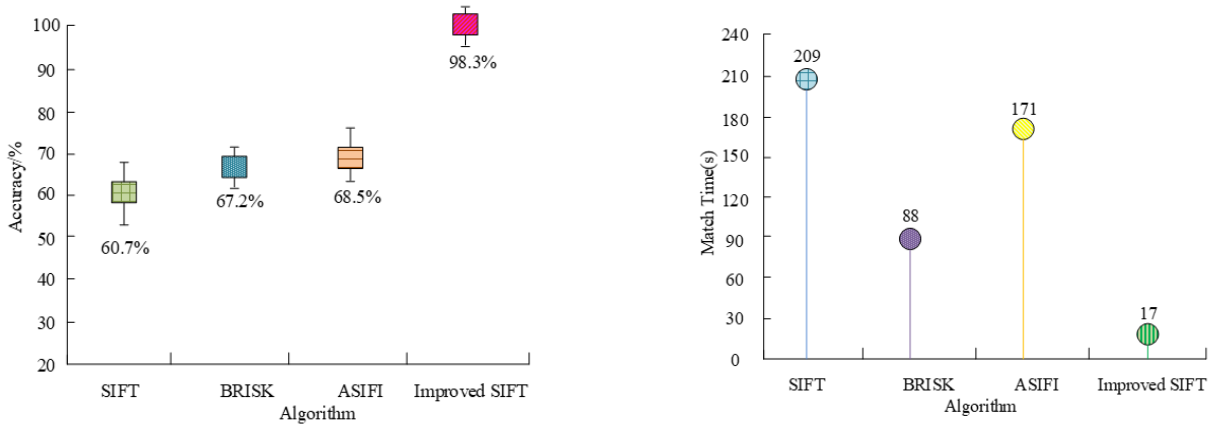

(a) Matching Accuracy of Four Algorithm

(b) Matching Time of Four Algorithm

Fig. 4.1: Comparison results of matching accuracy and time of four algorithms

modified SIFT algorithm reached a maximum of 57%. This indicated that the improved SIFT algorithm had more significant performance advantages.

The study continued with the selection of two buildings in a region as the objects, and feature matching was performed separately. The data were collected and processed for both buildings together. Figure 4.3 shows the results. In Figure 4.3a, the different circle patterns indicate the quantity of the valid matching points for building A, the rectangular pattern indicates the quantity of the matching points. Figure 4.3b shows the accuracy of matching points for building B. From Figure 10(a), the total matching points quantity of the traditional SIFT algorithm for building A was about 264, and the number of valid points was only 201. BRISK had more valid points but the total matching points quantity was lower than ASIFT. The improved SIFT algorithm, on the other hand, had the highest number of matching points and had 326 valid points. From Figure 10(b), the accuracy of matching points in building B for ASIFI, classical SIFT, BRISK, and the improved SIFT were 53.4%, 75.3%, 60.8%, and 96.2%, respectively, with the improved SIFT method improving by 30% on average compared to the first three. In Figure 4.3c, the improved SIFT algorithm took 23s and 47s for data acquisition and processing, respectively, with an accuracy rate of 97.2%, which was significantly better than the remaining three algorithms.

Three common classification models were chosen for comparison, namely Random Forest (RF), Logistic Regression (LR), and Support Vector Machine (SVM), to verify the classification effectiveness of the improved MVCNN on 3D building model data. The datasets chosen for the study were UrbanScene3D and MSBuilding, and the F1 value and accuracy rate were used as classification evaluation metrics. Figure 4.4 shows the classification results of the four algorithms. In Figure 4.4, the improved MVCNN model had the best F1 value and accuracy rate on both datasets compared to the other three models. In particular, the improved MVCNN achieved an F1 value of 96.4% and an accuracy of 97.6% on the UrbanScene3D dataset, which was 20.2% and 13.5% higher than RF, respectively. In the MSBuilding dataset, the model had the highest F1 value of 86.8% and accuracy of 87.7%, which were 15% and 9.6% higher than the LR model, respectively. This indicated that the improved MVCNN model had significant performance advantages in the data classification of 3D building models. The study continued to validate the classification effect of the improved MVCNN model on 3D building models by selecting six categories of 3D building models for experimental validation. A total of 10 sets of tests were conducted in the study to ensure the validity of the test results. Meanwhile, a traditional CNN was chosen for comparison. Figure 4.5 shows the test results. In Figure 4.5, the improved MVCNN model outperformed the classical CNN model in the classification of the 3D model for each category. Among them, the improved MVCNN achieved the highest classification accuracy of 94.26% in model 3, an improvement of 11.57% compared

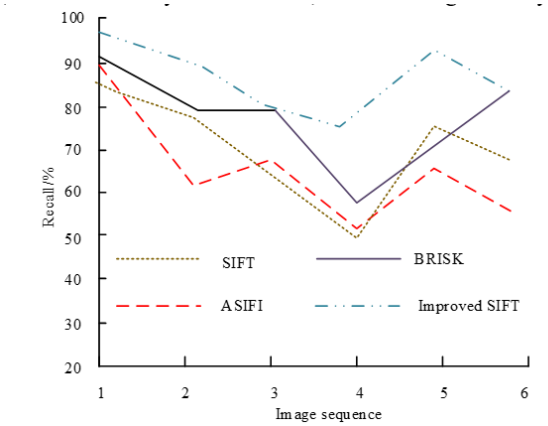

(a) The Recall of Four Algorithm

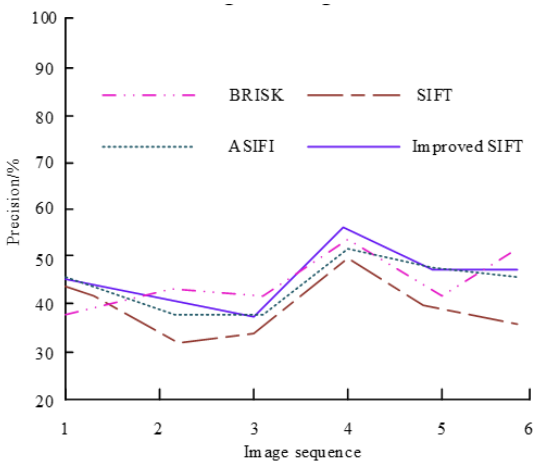

(b) Precision Results of Four Algorithm

Fig. 4.2: The recall and precision results of four methods

Table 4.2: Comparison results of different RMSE algorithms

Algorithm	Data set									
	UrbanScene3D					MSBuilding				
	Number of experiments					Number of experiments				
	1	2	3	4	5	1	2	3	4	5
CA	7.91%	10.82%	11.43%	8.95%	10.77%	9.32%	10.58%	12.79%	11.21%	9.68%
CART	6.55%	7.43%	8.95%	8.21%	7.32%	8.42%	7.38%	7.64%	8.77%	9.49%
KNN	7.59%	9.42%	10.67%	8.37%	7.11%	7.61%	8.73%	8.92%	10.85%	9.19%
ESNN	5.78%	6.42%	5.88%	7.01%	5.95%	6.35%	5.70%	7.03%	6.47%	6.51%
MVCNN	4.99%	4.03%	5.09%	4.27%	3.99%	4.86%	4.67%	4.12%	5.04%	4.65%
Improved MVCNN	2.51%	2.17%	2.58%	2.12%	1.89%	1.12%	1.37%	2.08%	1.94%	2.17%

to CNN. Meanwhile, the improved MVCNN achieved the highest classification accuracy of 75.09% in model 6, an improvement of 25.24% compared to CNN. The complexity of the 3D model determined the accuracy of the classification. Among them, model 3 was the simplest and therefore its accuracy was the highest, with an improvement of 19.17% and 32.84%, respectively, on the two classification models compared to the most complex model 6. This indicated that the improved MVCNN model was more accurate and stable in terms of classification accuracy.

Other algorithms were added for comparison to further validate the performance of the improved MVCNN model designed by the research. Comparison algorithms include Convolutional Autoencoder (CA)-based unsupervised noise rejection method, Classification and Regression Tree (CART), K-Nearest Neighbor (KNN), and Evolutionary Spike Neural Network (ESNN). The Root Mean Square Error (RMSE) index was used to better reflect the classification performance of the algorithm designed by the research on 3D building models. The dataset used in the experiment was also UrbanScene3D and MSBuilding. The comparison results of different RMSE algorithms are shown in Table 4.2.

From Table 4.2, the maximum RMSE of the improved MVCNN algorithm was 2.58% on the UrbanScene3D dataset, while the minimum RMSE values of CA, CART, KNN, ESNN, and MVCNN were 7.91%, 6.55%, 7.11%, 5.78%, and 3.99%, respectively. The maximum RMSE value of the improved MVCNN algorithm was significantly smaller than the minimum value of the comparison algorithms. The minimum RMSE values

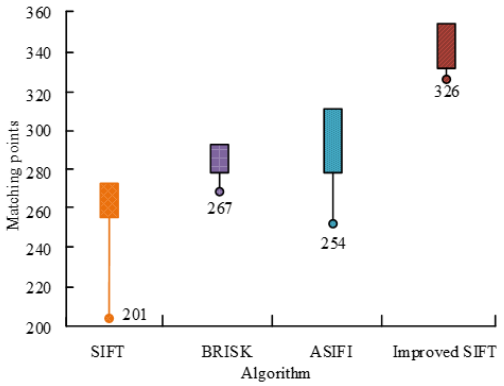

(a) Matching Point Results of Building A

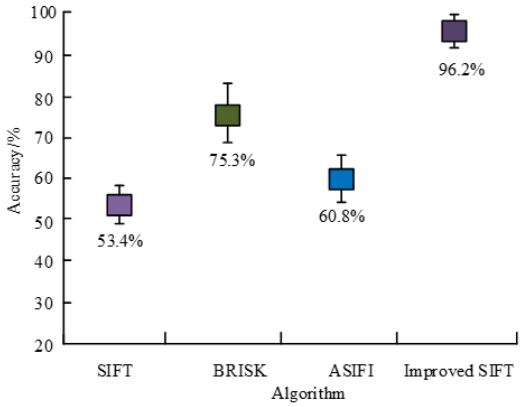

(b) Matching Point Results of Building B

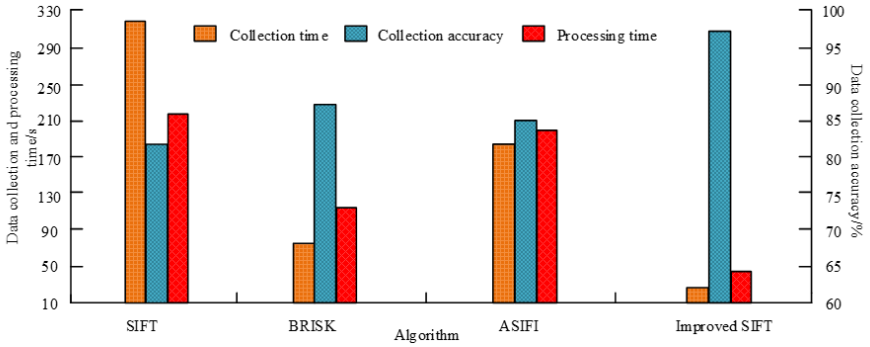

(c) Data Collection and Processing Results

Fig. 4.3: Data collection and processing results of four methods

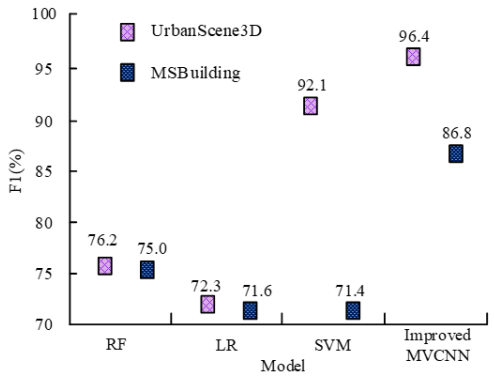

(a) F1 Values of Different Models on the Dataset

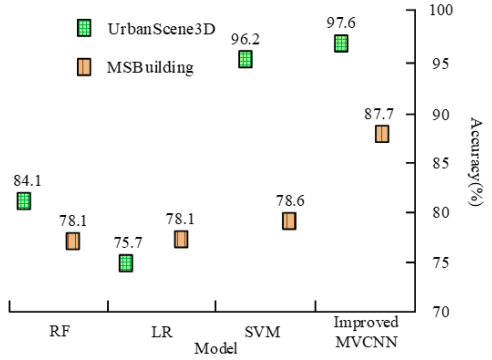

(b) Accuracy Values of Different Models on the Dataset

Fig. 4.4: Classification results of four algorithms

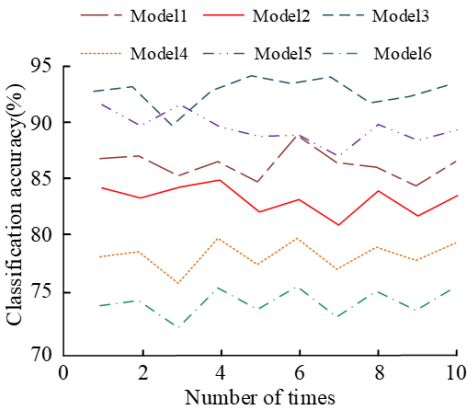

(a) Classification Results of Improved MVCNN model

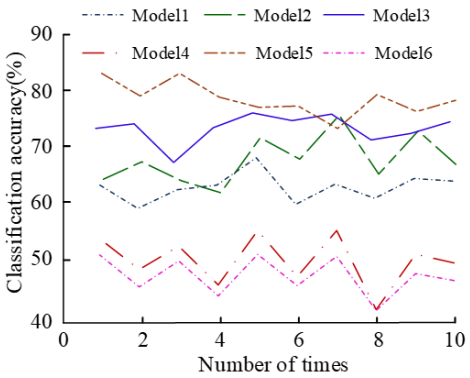

(b) Accuracy Values of Different Models on the Dataset

Fig. 4.5: Classification Results of CNN model

Table 4.3: Comparison of time consumption and CPU utilization of different algorithms

Algorithm	Time consuming					CPU utilization				
	Number of experiments					Number of experiments				
	1	2	3	4	5	1	2	3	4	5
CA	67.1s	78.9s	89.8s	77.7s	76.5s	27.2%	25.7%	23.8%	21.7%	22.3%
CART	58.4s	57.1s	54.0s	53.7s	54.4s	19.0%	17.8%	15.7%	18.2%	15.5%
KNN	51.7s	49.8s	48.3s	48.1s	50.4s	18.5%	16.4%	17.2%	16.2%	18.6%
ESNN	48.7s	46.5s	43.2s	41.9s	41.7s	15.8%	14.7%	16.3%	15.9%	14.1%
MVCNN	36.8s	35.4s	36.9s	35.3s	35.5s	13.2%	12.5%	13.1%	12.9%	13.6%
Improved MVCNN	18.9s	21.3s	19.1s	18.2s	18.0s	11.2%	10.0%	11.6%	10.8%	9.8%

of CA, CART, KNN, ESNN, and MVCNN were 9.32%, 7.38%, 7.61%, 5.70%, and 4.12%, respectively, on the MSBuilding dataset. The maximum RMSE value of the improved MVCNN algorithm was 2.17%, which was significantly smaller than the minimum values of the comparison algorithms. Therefore, the improved MVCNN algorithm had smaller classification errors and better performance. A comparison was conducted on the classification time and CPU utilization of different algorithms to further verify the performance of the improved MVCNN algorithm. The comparison results are shown in Table 4.3.

From Table 4.3, the maximum classification time of the improved MVCNN algorithm was 21.3 seconds, while the maximum classification time of CA, CART, KNN, ESNN, and MVCNN was 89.8s, 58.4s, 51.7, 48.7, and 36.9, respectively. The classification time of the improved MVCNN algorithm was significantly lower than that of the comparison algorithm. The maximum CPU utilization of the improved MVCNN algorithm was 11.6%, while the maximum CPU utilization of CA, CART, KNN, ESNN, and MVCNN was 27.2%, 19.0%, 18.6%, 16.3%, and 13.6%, respectively. The CPU utilization of the improved MVCNN algorithm was significantly lower than that of the compared algorithms. Therefore, the improved MVCNN algorithm had the shortest time consumption, the lowest CPU utilization, and better performance.

5. Simulation result and discussion. With the development of intelligent building technology, it is gradually being applied to various aspects of the construction field, promoting the informatization development of intelligent buildings [15]. An intelligent building 3D information management system combining BIM and GIS technologies was studied and designed to efficiently manage the 3D information of intelligent buildings. An

improved SIFI algorithm was adopted for feature extraction and matching of 3D information to further enhance the management ability of the system for massive information data, and the improved MVCNN algorithm was used to classify 3D information. It was found that the SIFI algorithm could accurately match 3D building information and had good performance. This is consistent with the research findings of Attila Fej é r and other experts. Experts such as Attila Fej é r used SIFI to detect the coordinates of the transformed objects and improved the SIF algorithm. The research results showed that the average accuracy and recall values of the SIFI algorithm were 0.84 and 0.94, respectively, indicating its good performance in the fields of detection and matching (Attila et al. 2021). In addition, the improved MVCNN algorithm performed well in information classification, with the highest accuracy reaching 97.6%. This is consistent with the research findings of Starly B et al. Starly B et al. used the MVCNN algorithm and transfer learning to classify and retrieve the shapes of computer-aided design models. The research results showed that the MVCNN algorithm could efficiently classify shapes with a classification accuracy of up to 93% [29, 43, 44, 45]..

6. Conclusion. BIM and GIS technologies were combined to construct 3D IM systems to improve the intelligent buildings management. IM was mainly implemented through the improved SIFT algorithm and the improved MVCNN algorithm. According to the findings, the improved SIFT achieved the highest matching accuracy and was as high as 98.3%. Their matching accuracy rates were improved by 29.8%, 31.1%, and 37.6%, respectively, compared with the remaining three algorithms. The difference between ASIFI and the classical SIFT algorithm was small by comparing the full search rate, with the lowest being around 50% and the highest close to 90%, and the overall trend was first decreasing and then increasing. The improved SIFT algorithm was able to maintain a completion rate of over 78% and reached a maximum of 97%, a maximum improvement of 42% compared to the improved SIFT algorithm. On the UrbanScene3D dataset, the improved MVCNN achieved an F1 value of 96.4% and an accuracy of 97.6%, which was 20.2% and 13.5% higher than RF, respectively. In the MSBuilding dataset, the model had the highest F1 value of 86.8% and accuracy of 87.7%, which were 15% and 9.6% higher than the LR model, respectively. This indicated that the improved MVCNN model had significant performance advantages in the data classification of 3D building models. In summary, the proposed 3D IM method has a high accuracy rate and can effectively improve the management of intelligent buildings. However, the study does not make use of systematic data pre-processing measures in the management of 3D information of intelligent buildings. Therefore, pre-processing methods such as data conversion need to be expanded to further optimise it.

REFERENCES

[1] Asgari, S., Sarvari, H., Chan, D., Chan, D., Nassereddine, H. & Chen, Z. A multi-criteria optimization study for locating industrial warehouses with the integration of BIM and GIS data. *Architectural Engineering And Design Management*. **17**, 478-495 (2021)

[2] Attila, F. Zoltán. *Nagy, Benois-Pineau. Jenny, Péter. Szolgay, A. D. Rugy, And Domenger. Jean-Philippe "Implementation Of Scale Invariant Feature Transform Detector On Fpga For Low-power Wearable Devices For Prostheses Control*. **49**, 2255-2273 (2021), https://doi.org/10.1002/cta.3025

[3] Bo, J., Lei, L., Sheng, Z., Shan-Shan, Y., Shu-Guang, Z. & Yao, H. An automatic detection for solar active regions based on scale-invariant feature transform and clustering by fast search and find of density peaks. *Chinese Astronomy And Astrophysics*. **46**, 264-276 (2022), https://doi.org/10.1016/j.chinastron.2022.09.007

[4] Bansal, G., Muzatko, S. & Shin, S. Information system security policy noncompliance: the role of situation-specific ethical orientation. *Information Technology & People*. **34**, 250-296 (2020), https://doi.org/10.1108/ITP-03-2019-0109

[5] Chen, Z. Research on internet security situation awareness prediction technology based on improved RBF neural network algorithm. *Journal Of Computational And Cognitive Engineering*. **1**, 103-108 (2022), https://doi.org/10.47852/bonviewJCCE149145205514

[6] Cherif, K., Yamina, B. & And, B. Lahsen. *Wahib Kébir "Delineation Of Groundwater Potential Zones In Wadi Saida Watershed Of Nw-algeria Using Remote Sensing, Geographic Information System-based Ahp Techniques And Geostatistical Analysis*. **9**, 45-64 (2021), https://doi.org/10.19637/j.cnki.2305-7068.2021.01.005

[7] Dinis, F., Poças, M., Guimarães, A. & Rangel, B. BIM and semantic enrichment methods and applications: a review of recent developments. *Archives Of Computational Methods In Engineering*. **29**, 879-895 (2022), https://doi.org/10.1007/s11831-021-09595-6

[8] Hosseini, H. & Taleai, M. A Review of Recent Researches on Integration of Building Information Modeling (BIM) and GIS. *Iranian Journal Of Remote Sensing & GIS*. **13**, 33-58 (2021), https://doi.org/10.52547/gisj.13.3.33

[9] Hassan, T., Fath-Allah, T., Elhabiby, M., Awad, E. & El-Tokhey, M. Integration of gnss observations with volun-

teered geographic information for improved navigation performance. *Journal Of Applied Geodesy*. **16**, 265-277 (2022), https://doi.org/10.1515/jag-2021-0063

[10] Huo, Y., Liu, T., Yang, Y., Ma, C. & Ni., X. In situ measurement of 3d crystal size distribution by double-view image analysis with case study on l-glutamic acid crystallization. *Industrial & Engineering Chemistry Research*. **59**, 4646-4658 (2020), https://doi.org/10.1021/acs.iecr.9b05828

[11] Khaleghi, F., Alizadeh, S. & Azizi, M. Integration of Building Information Modeling (BIM) and Geographic Information System (GIS) to Develop a Smart City. *Naqshejahan-Basic Studies And New Technologies Of Architecture And Planning*. **12**, 46-73 (2022)

[12] Kaczorek, T. & Ruszewski, A. Global stability of discrete-time feedback nonlinear systems with descriptor positive linear parts and interval state matrices. *International Journal Of Applied Mathematics And Computer Science*. **32**, 5-10 (2022), https://doi.org/10.34768/amcs-2022-0001

[13] Kaiwen, J., Jian, L., Tongtong, X., Shujing, L., Shunyao, W. & Fengjing, S. Power-law initialization algorithm for convolutional neural networks. *Neural Computing & Applications*. **35**, 22431-22447 (2023), https://doi.org/10.1007/s00521-023-08881-7

[14] Kaur, J. & Singh, J. Roman to gurmukhi social media text normalization. *International Journal Of Intelligent Computing And Cybernetics*. **13**, 407-435 (2020), https://doi.org/

[15] Liu, H. A simplified relationship between the modified o-lattice and the rotation matrix for generating the coincidence site lattice of an arbitrary bravais lattice system. *Acta Crystallographica. Section A, Foundations And Advances*. **78**, 139-148 (2022), https://doi.org/10.1107/S2053273322000171

[16] Luo, H., Jiang, W., Gu, Y., Liu, F., Liao, X. & Lai, S. A strong baseline and batch normalization neck for deep person re-identification. *IEEE Transactions On Multimedia*. **22**, 2597-2609 (2020), https://doi.org/10.1109/TMM.2019.2958756

[17] Li, J., Liu, W., Zhang, Y., He, S., Kong, F. & Li., R. The application of iot technology in energy management of intelligent building. *Journal Of Mines, Metals & Fuels*. **70**, 315-324 (2022), https://doi.org/10.18311/jmmf/2022/30804

[18] Law, S., Seresinhe, C., Shen, Y. & Gutierrez-Roig, M. Street-Frontage-Net: urban image classification using deep convolutional neural networks. *International Journal Of Geographical Information Science*. **34**, 681-707 (2020), https://doi.org/10.1080/13658816.2018.1555832

[19] Moll, T. Six days in plastic: potentiality, normalization, and in vitro embryos in the postgenomic age. *Science, Technology, & Human Values*. **47**, 1253-1276 (2022), https://doi.org/10.1177/01622439221090685

[20] Mazlana, M., Mauluda, K., Rahmanc, S., Bahrid, M. & Rahmand, M. Emergency Management in Building Based On 3D BIM and GIS Technology. *Jurnal Kejuruteraan*. **34**, 1215-1228 (2022), https://doi.org/10.17576/jkukm-2022-34(6)-22

[21] Mahamood, S. & Fathi, M. Seismic building design work process using building information modeling (BUM) technology for Malaysian Government projects. *International Journal Of Disaster Resilience In The Built Environment*. **13**, 211-232 (2022), https://doi.org/10.1108/IJDRBE-10-2021-0135

[22] Moballeghi, E., Pourrostam, T., Abbasianjahromi, H. & Makvandi, P. Assessing the effect of building information modeling system (bim) capabilities on lean construction performance in construction projects using hybrid fuzzy multi-criteria decision-making methods. (2023)

[23] Science, I. & Technology, T. of Civil Engineering 47(3): 1871-1891. *Meng, Q., Y. Zhang, Z. Li, W. Shi, J. Wang, Y. Sun, And X. Wang "A Review Of Integrated Applications Of BIM And Related Technologies In Whole Building Life Cycle*. **27**, 9-2019 (2020), https://doi.org/10.1007/s40996-022-00971-1

[24] Pathak, Y., Shukla, P., Tiwari, A., Stalin, S. & Singh, S. Deep transfer learning based classification model for COVID-19 disease. *Irbm*. **43**, 87-92 (2022), https://doi.org/10.1016/j.irbm.2020.05.003

[25] Rathore, N. Umashankar. *Rawat, Satish. Chandra. Kulhari "Efficient Hybrid Load Balancing Algorithm." National Academy Science Letters (Q-3), Publication 43(2*. pp. 177-185 (2020)

[26] Qi, J., Wu, Q., Zhang, Y., Weng, G. & Zhou, D. Unified residue method for design of compact wide-area damping controller based on power system stabilizer. *Journal Of Modern Power Systems And Clean Energy*. **8**, 367-376 (2020), https://doi.org/10.35833/MPCE.2018.000370

[27] Reddy, G., Deepika, K., Malliga, L., Hemanand, D., Senthilkumar, C. & Gopalakrishnan, S. Human action recognition using difference of gaussian and difference of wavelet. *Big Data Mining And Analytics*. **6**, 336-346 (2023), https://doi.org/10.26599/BDMA.2022.9020040

[28] Stewart, H. A systematic framework to explore the determinants of information security policy development and outcomes. *Information & Computer Sceurity*. **30**, 490-516 (2022), https://doi.org/10.1108/ICS-06-2021-0076

[29] Starly, B., Angrish, A. & Bharadwaj, A. Mvcnn++: cad model shape classification and retrieval using multi-view convolutional neural networks. *Journal Of Computing And Information Science In Engineering*. **21**, 1-27 (2020), https://doi.org/10.1115/1.4047486

[30] Stride, M., Hon, C., Liu, R. & Xia, B. The use of building information modelling by quantity surveyors in facilities management roles. *Engineering*. **27**, 1795-1812 (2020), https://doi.org/10.1108/ECAM-11-2019-0660

[31] Sawant, S. & Manoharan, P. Unsupervised band selection based on weighted information entropy and 3D discrete cosine transform for hyperspectral image classification. *International Journal Of Remote Sensing*. **41**, 3948-3969 (2020)

[32] Su, Y., Li, J., Li, W., Gao, Z., Chen, H., Li, X. & Liu, A. Semantically guided projection for zero-shot 3D model classification and retrieval. *Multimedia Systems*. **28**, 2437-2451 (2022), https://doi.org/10.1007/s00530-022-00970-2

[33] Xing, Z., Jianhao, B. & Yinghua, F. Change detection based on tensor robust principal component analysis for retinal fundus image serial. *Information And Control*. **52**, 115-128 (2023), https://doi.org/10.13976/j.cnki.xk.2023.2131

[34] Yang, D., Guo-ru, L., Meng-cheng, R. & Hong-yang, P. Retinal blood vessel segmentation method based on multi-scale convolution kernel u-net model. *Journal Of Northeastern University(Natural Science)*. **42**, 7-14 (2021), https://doi.org/10.12068/j.issn.1005-3026.2021.01.002

[35] Zhang, C., Wang, J., Tang, S., Wang, D., Yin, X. & Shuai, Z. A new pfc design with interleaved mhz-frequency gan auxiliary active filter phase and low-frequency base power si phase. *IEEE Journal Of Emerging And Selected Topics In Power Electronics*. **8**, 557-566 (2020), https://doi.org/10.1109/JESTPE.2019.2955960

[36] Zhang, M., You, H., Kadam, P., Liu, S. & Kuo, C. Pointhop: An explainable machine learning method for point cloud classification. *IEEE Transactions On Multimedia*. **22**, 1744-1755 (2020)

[37] Zhao, L., Mbachu, J. & Liu, Z. Developing an Integrated BIM+ GIS Web-Based Platform for a Mega Construction Project. *KSCE Journal Of Civil Engineering*. **26**, 1505-1521 (2022), https://doi.org/10.1007/s12205-022-0251-x

[38] Zheng, B., Gao, A., Huang, X., Li, Y., Liang, D. & Long, X. A modified 3D EfficientNet for the classification of Alzheimer's disease using structural magnetic resonance images. *IET Image Processing*. **17**, 77-87 (2023), https://doi.org/10.1049/ipr2.12618

[39] Zhu, J., Tan, Y., Wang, X. & Wu., P. BIM/GIS integration for web GIS-based bridge management. *Annals Of GIS*. **27**, 99-109 (2021), https://doi.org/10.1080/19475683.2020.1743355

[40] Zhang, T. & Deng, C. Technical repair method of poyang bodiless lacquerware based on scale-invariant feature transform algorithm for healthcare vision. *Journal Of Testing And Evaluation: A Multidisciplinary Forum For Applied Sciences And Engineering*. **51**, 315-326 (2023), https://doi.org/10.1520/JTE20210460

[41] Zhong, J., Qu, Z., Tang, Y. & Pan, Y. Continuous and discrete similarity coefficient for identifying essential proteins using gene expression data. *Big Data Mining And Analytics*. **6**, 185-200 (2023), https://doi.org/10.26599/BDMA.2022.9020019

[42] Zhou, X., Xie, Q., Guo, M., Zhao, J. & Wang, J. Accurate and efficient indoor pathfinding based on building information modelling data. *IEEE Transactions On Industrial Informatics*. **16**, 7459-7468 (2020), https://doi.org/10.1109/TII.2020.2974252

[43] Hussain, K., Hussain, S., Jhanjhi, N. & Humayun, M. SYN flood attack detection based on bayes estimator (SFADBE) for MANET. *2019 International Conference On Computer And Information Sciences (ICCIS)*. pp. 1-4 (2019)

[44] Lim, M., Abdullah, A., Jhanjhi, N. & Supramaniam, M. Hidden link prediction in criminal networks using the deep reinforcement learning technique. *Computers*. **8**, 8 (2019)

[45] Kumar, T., Pandey, B., Musavi, S. & Zaman, N. CTHS Based Energy Efficient Thermal Aware Image ALU Design on FPGA Springer Wireless Personal Communications. *An International Journal, ISSN*. pp. 0929-6212 (2015)

Edited by: Zhengyi Chai
Special issue on: Data-Driven Optimization Algorithms for Sustainable and Smart City
Received: Nov 30, 2023
Accepted: Feb 23, 2024